Direct visualization of phosphorylase—phosphorylase kinase complexes by scanning tunneling and atomic force microscopy

Ronald D. Edstrom,* Marilyn H. Meinke,* Xiuru Yang,*‡ Rui Yang,‡ Virgil Elings,§ and D. Fennell Evans§

*Department of Biochemistry, Medical School, and ‡Center for Interfacial Engineering, Institute of Technology, University of Minnesota, Minneapolis, Minnesota 55455; and §Digital Instruments, Santa Barbara, California 93117 USA

ABSTRACT In skeletal muscle the activation of phosphorylase *b* is catalyzed by phosphorylase kinase. Both enzymes occur in vivo as part of a multienzyme complex. The two enzymes have been imaged by atomic force microscopy and the results compared to those previously found by scanning tunneling microscopy. Scanning tunneling microscopy and atomic force microscopy have been used to view complexes between the activating enzyme phosphorylase kinase and its substrate phosphorylase *b*. Changes in the size and shape of phosphorylase kinase were obseved when it bound phosphorylase *b*.

INTRODUCTION

One of the goals of biochemistry is to understand the interactions between enzymes that control life processes. Whereas we have obtained direct structural information on many enzymes from x-ray crystallography, electron microscopy, and scanning tunneling microscopy, almost all of our information on the structure of enzyme complexes comes from inferences derived from indirect measurements. In this report, we provide images of two enzymes, phosphorylase *b* and phosphorylase kinase, in their isolated and complexed states. Direct visualization with atomic force microscopy (AFM)[1] and scanning tunneling microscopy (STM) permits changes in size and shape of phosphorylase kinase upon complex formation with phosphorylase *b* to be determined. We have shown that AFM and STM provide complementary information on the structure of biomacromolecules.

Muscle glycogenolysis is controlled by the combined influence of neuronal and hormonal regulation. After a series of signal transduction processes, a phosphate is transferred from Mg-ATP to phosphorylase *b*, by phosphorylase kinase. Both of these proteins have been studied by STM (1, 2) and the images were seen to have structural features similar to those found by x-ray crystallography (3) and electron microscopy (4–6). Phosphorylase *b* (M_r 97,500) which occurs in dilute solution as dimers or tetramers (7) was found to form linear chains of dimers when applied to the graphite surface used to hold the sample during STM. Phosphorylase kinase (M_r 1.3×10^6) is a hexadecamer of four copies each of four different subunits (α, β, γ, δ) (8). Images of this enzyme showed single bilobate molecules corresponding to a dimer of octamers (4). During the catalytic event, the γ-subunits of phosphorylase kinase bind phosphorylase *b* to form an enzyme-substrate complex (9, 10). The stoichiometry of this complex during catalysis is not known although with four catalytic subunits the kinase may bind up to four phosphorylase *b* molecules. Under nonphysiological, dilute conditions, only two phosphorylase *b* have been

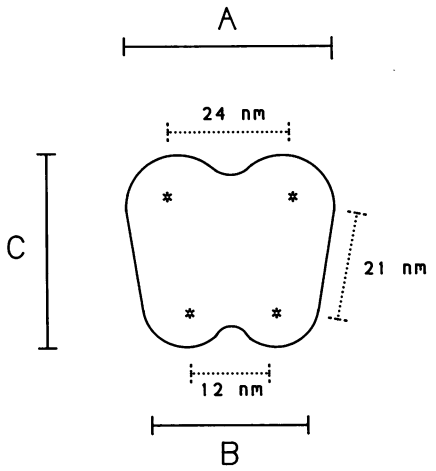

FIGURE 1 Representation of phosphorylase kinase with dimensions listed in Table 1. The numbers on the dotted lines are the values reported previously (1). The end points of those lines were at the place where tangent lines left the perimeter of the molecules. We found it more useful to use the dimensions labeled *A*, *B*, and *C* for the calculations presented in this report. The asterisks indicate the approximate position of the height measurements. The diagram is not drawn to scale.

Address correspondence to Dr. R. D. Edstrom, Department of Biochemisty, 4-225 Millard Hall, University of Minnesota, Minneapolis, MN 55455; (612) 625-0931 or fax (612) 625-2163.

[1]*Abbreviations used in this paper:* AFM, atomic force microscopy; HOPG, highly ordered pyrolytic graphite; STM, scanning tunneling microscopy.

0006-3495/90/12/1437/12 $2.00

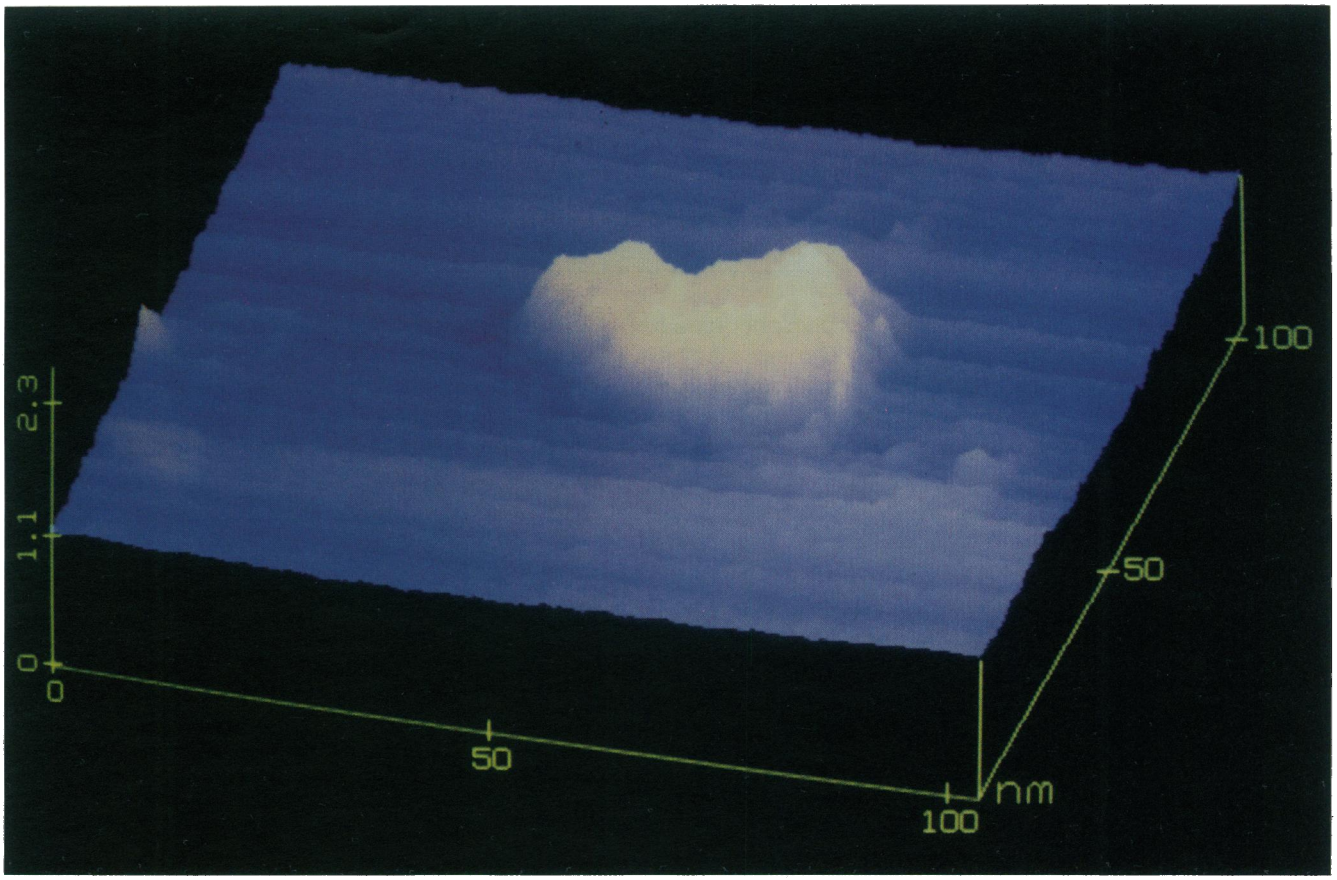

FIGURE 2 Images of individual phosphorylase kinase molecules by STM (*A*) and AFM (*B*). The enzyme was applied to the graphite surface and scanned as described in Experimental Procedures.

reported to be bound to the enzyme (11). Reaction mechanism studies showed that the binding of phosphorylase *b* and Mg-ATP to phosphorylase kinase is either random (12) or ordered bi-bi (13). At high concentrations of the proteins, a complex between phosphorylase kinase and phosphorylase *b* should be observable in either case.

The near field techniques of STM (14) and AFM (15) depend on probes with tips of atomic dimensions scanning the surface of an object while a computer maintains a constant height or tunneling current for STM, or force between the probe and the surface in the case of AFM. The feedback signal in STM is an electrical tunneling current passing from the wire probe through the sample to the underlying conductive surface. In AFM, the signal is a force between the surface being imaged and a sharp diamond shard mounted on a mirrored cantilever. The position of the cantilever is reported to the computer by a reflected laser beam. Both techniques are capable of providing images with resolution at the atomic level for conducting, crystalline materials. They are presented here as methods of visualizing protein molecules and their complexes.

EXPERIMENTAL PROCEDURES

A Nanoscope II (Digital Equipment Inc., Santa Barbara, CA) was used for STM as described previously (1). AFM was performed using a Nanoscope FM and a diamond stylus probe (16). Phosphorylase *b* (17) and phosphorylase kinase (18) were prepared from rabbit muscle and stored in buffer (50% glycerol, 25 mM Hepes, 1 mM EDTA, 0.5 mM β-mercaptoethanol, and pH 7.0). Before use for imaging, the enzymes were dialyzed extensively against 20 mM Hepes, pH 7.0. Samples were applied to the graphite surface as described previously (1). In the cases where complexes were to be viewed, the proteins were mixed and incubated at room temperature for 2–5 min before applying to the graphite surface. Image measurements and data analysis were all carried out using the software provided with the instruments. STM bias potentials were between 80 and 120 mV and the current was set to between 0.4 and 0.6 nA. The D head was used with a mechanically sheared Pt/Ir (80/20) probe. Dimensions were obtained using cross sections of the images and measuring between the points where the first obvious increases in height occurred on each edge (Fig. 1). Thickness measurements were also made from cross sections. Four measurements

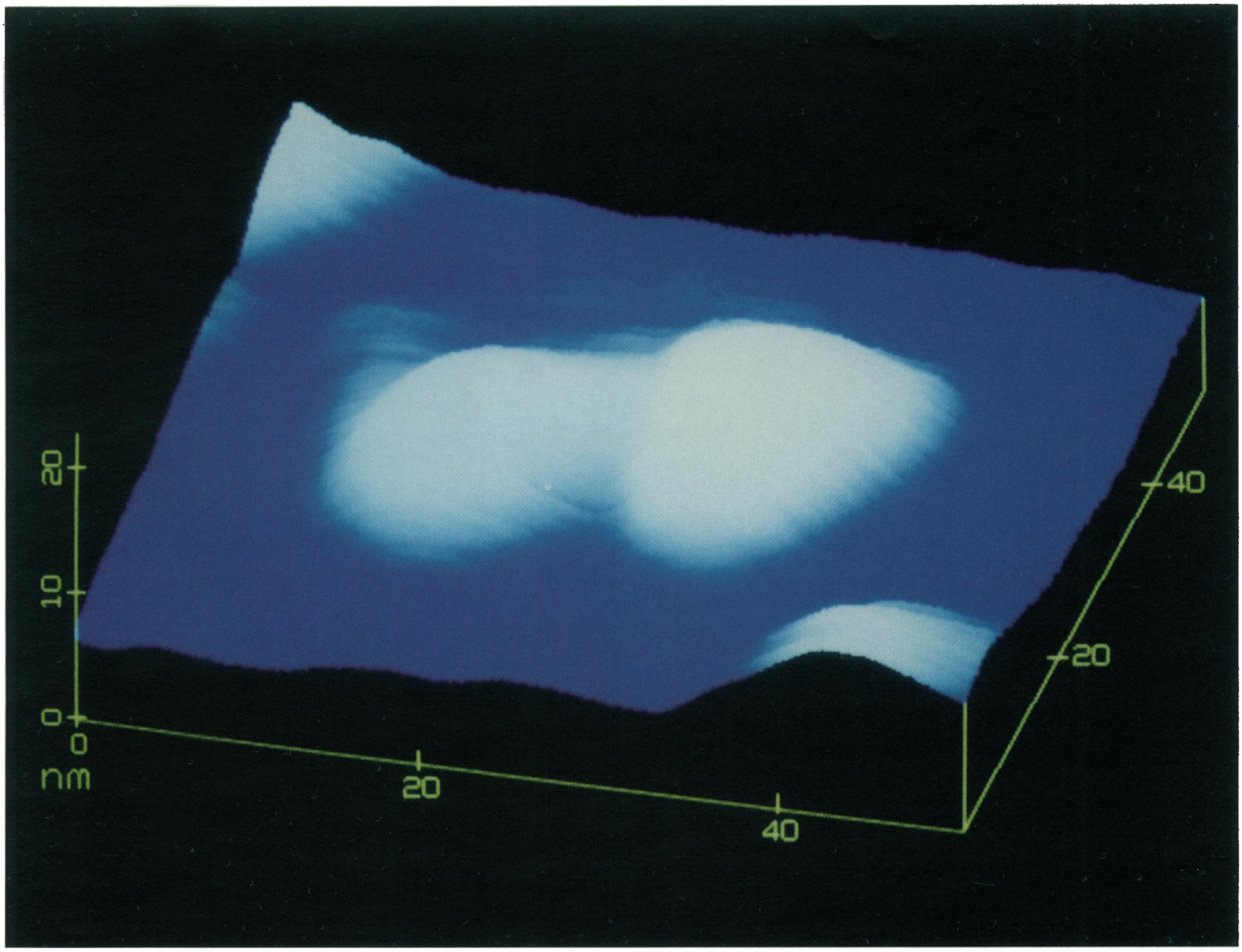

FIGURE 2 (continued)

were made near the "corners" of each molecule (as indicated in Fig. 1). The four values were ranked and the mean of the two central values was taken as the thickness of that molecule. Where reported, *n* values signify the number of individual molecules or complexes measured.

RESULTS AND DISCUSSION

Our primary goal in this report is to describe a complex formed by phosphorylase kinase and phosphorylase *b*. We first focus on the images and measurements of the individual enzymes. An understanding of their sizes and conformations provides a basis for interpretation of the images of the multienzyme complexes.

The visualizations of phosphorylase kinase obtained by AFM and STM are compared in Fig. 2. The STM image (Fig. 2 *A*) is a representative view of the molecule showing the butterfly shape and central depression described previously (1). An example of an AFM image of phosphorylase kinase can be seen in Fig. 2 *B*. This image is typical of AFM images we have obtained which lack the

TABLE 1 Measurements of phosphorylase kinase by STM and AFM

	*A**	*B*	*C*	*Height*	*Area*	*Volume*
	nm	*nm*	*nm*		nm^2	nm^3
STM ($n = 4$)	36 (35–37)‡	22 (17–25)	27 (26–27)	0.69 (0.61–0.72)	780	540
AFM ($n = 6$)	32 (28–37)	23 (16–32)	22 (21–26)	5.9 (4.7–6.9)	605	3570

*Letters refer to dimensions on Fig. 1; ‡Ranges are in parentheses.

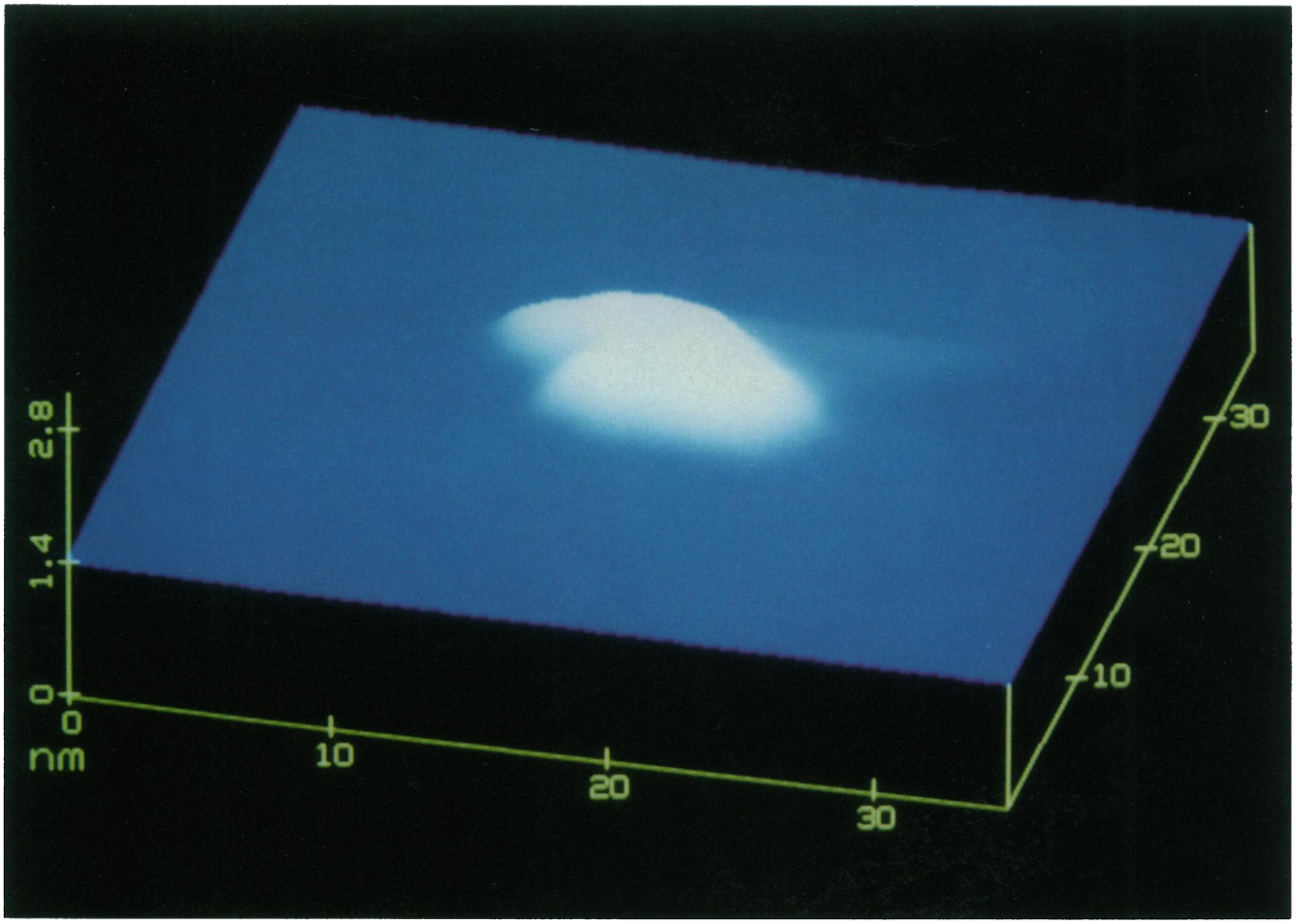

FIGURE 3 A phosphorylase tetramer as visualized by AFM.

apparent detail seen in the STM images of this protein although the overall shape and size are similar. In addition to the typical examples shown here we occasionally see what appear to be damaged molecules including those with partially separated lobes. These fragmented or distorted molecules are similar to those observed by electron microscopy (4). Measurement of the phosphorylase kinase molecules by the two techniques yielded the values in Table 1. The areas and volumes were calculated based on the simplifying assumptions of a trapezoidal shape and a uniform thickness. The volumes of 540 nm^3 (STM) and 3,570 nm^3 (AFM) are 0.3 and 2 times the calculated volume, V_h, which is 1,800 nm^3. This is obtained by assuming a partial specific volume ($\overline{V}_2$) of 0.74 cm^3/g (18), an extent of hydration of air-dried protein films corresponding to $\delta_1 = 0.4$ mol H_2O/mol amino acid (19) and a molecular weight, M, of 1.3×10^6 g/mol using

$$V_h = (M/N_0)(\overline{V}_2 + \delta_1 \overline{V}_1),$$

where N_0 is Avogadro's number, and $\overline{V}_1$ is the molar volume of water.

Neither STM nor AFM gives a molecular volume that is close to the calculated value. The lateral dimensions obtained by the two near field techniques are in reasonable agreement. The large differences in vertical dimensions reflect the difference in STM and AFM interactions with the specimens that are responsible for image generation. In STM, the feedback signal, which maintains constant separation between the tip and the sample, is determined by a combination of the physical dimensions and the interaction between the graphite substrate and the protein (20). With organic molecules the measured vertical distance is always found to be less than the actual physical dimension. For example, with DNA the diameter of the helix measured in the vertical dimension is 1.4 nm whereas the value obtained in the horizontal direction, 2.5 nm, agrees with x-ray data (21). Our thickness measurements of phosphorylase *b* molecules by STM yield an

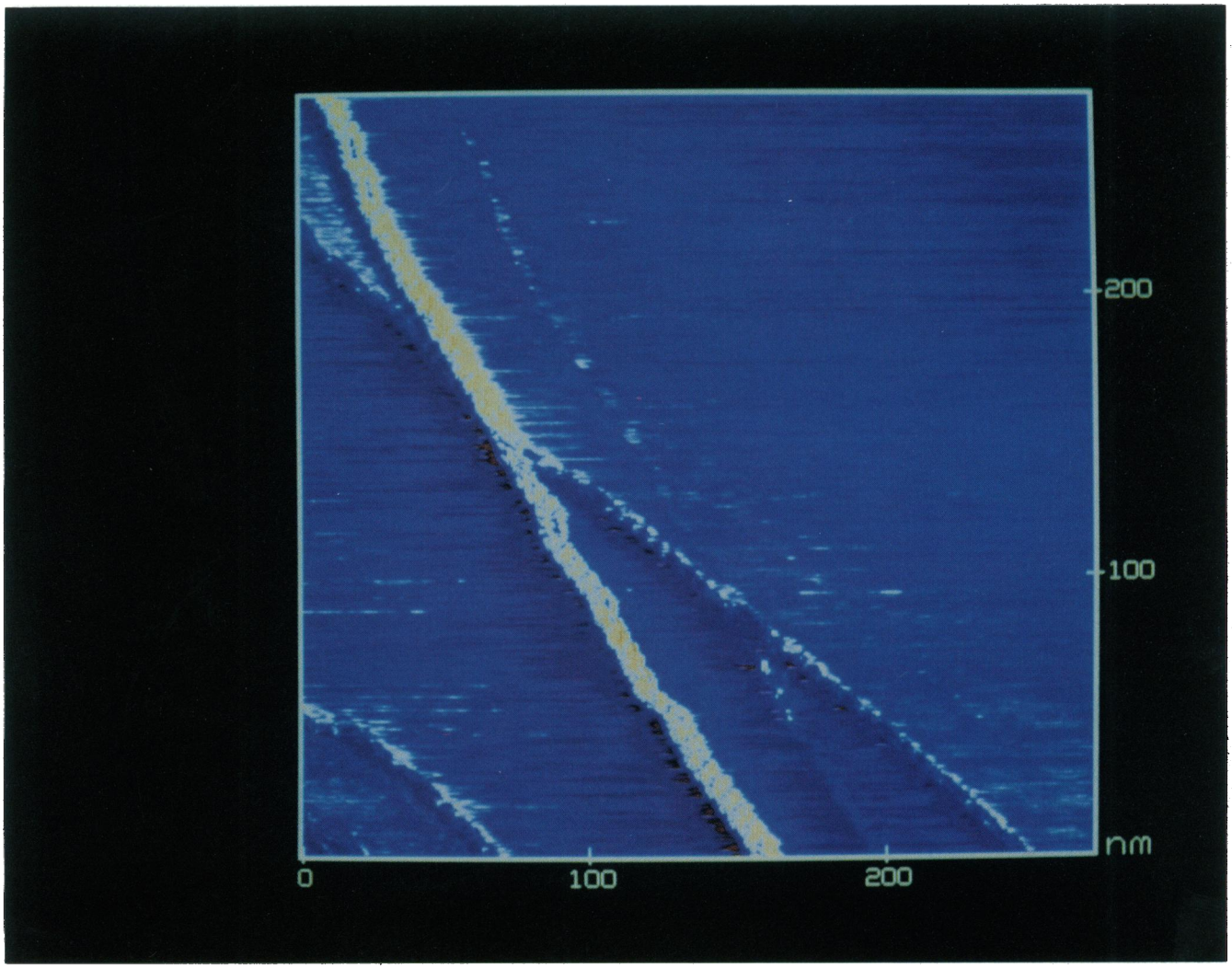

FIGURE 4 A short section of a chain of phosphorylase *b* dimers (*yellow*). The entire chain was several micrometers long. The chain is 11 nm wide and the repeat distance is 5.7 nm. The phosphorylase chain is seen to be crossing a ledge (*white*) on the graphite surface at left of center in the figure. A narrower scan on the cover of this issue shows six phosphorylase dimers at a higher magnification.

average value of 1.6 ± 0.2 nm ($n = 8$). X-Ray scattering and electron microscopy studies indicate that the minimum dimension is ~5.5 nm (6, 22) giving an STM thickness that is only 30% of the established value. Because the basis for image production of these large insulating molecules is not known, it is not possible to explain the height discrepancy. For monolayers of small organic compounds, with thicknesses of <5 Å, it has been proposed that image contrast is caused by the permanent or induced polarization of the organic molecules modifying the local electrical work function of the graphite (20). It seems unlikely that large proteins with thicknesses of as much as 50 Å could be imaged by that mechanism. With AFM, the vertical dimension is determined by the displacement of the diamond stylus as it rasters across the sample's surface. If the deformability of the substrate (graphite) and the protein molecule are similar, the vertical displacement should be an accurate measure of the molecular height. The discrepancy between the volume measured by AFM and that calculated for phosphorylase kinase may be due to the inability of the AFM to resolve molecular substructure. AFM images of phosphorylase kinase are biolobar, slightly convex plates whose measured volumes would be in error by the amount of any such structural details that could not be detected. The present fabrication techniques for preparing and mounting AFM probes do not provide the level of image resolution we find with STM. AFM resolution could be lost because the diamond chip was not sufficiently sharp or not mounted in the optimal orientation on the cantile-

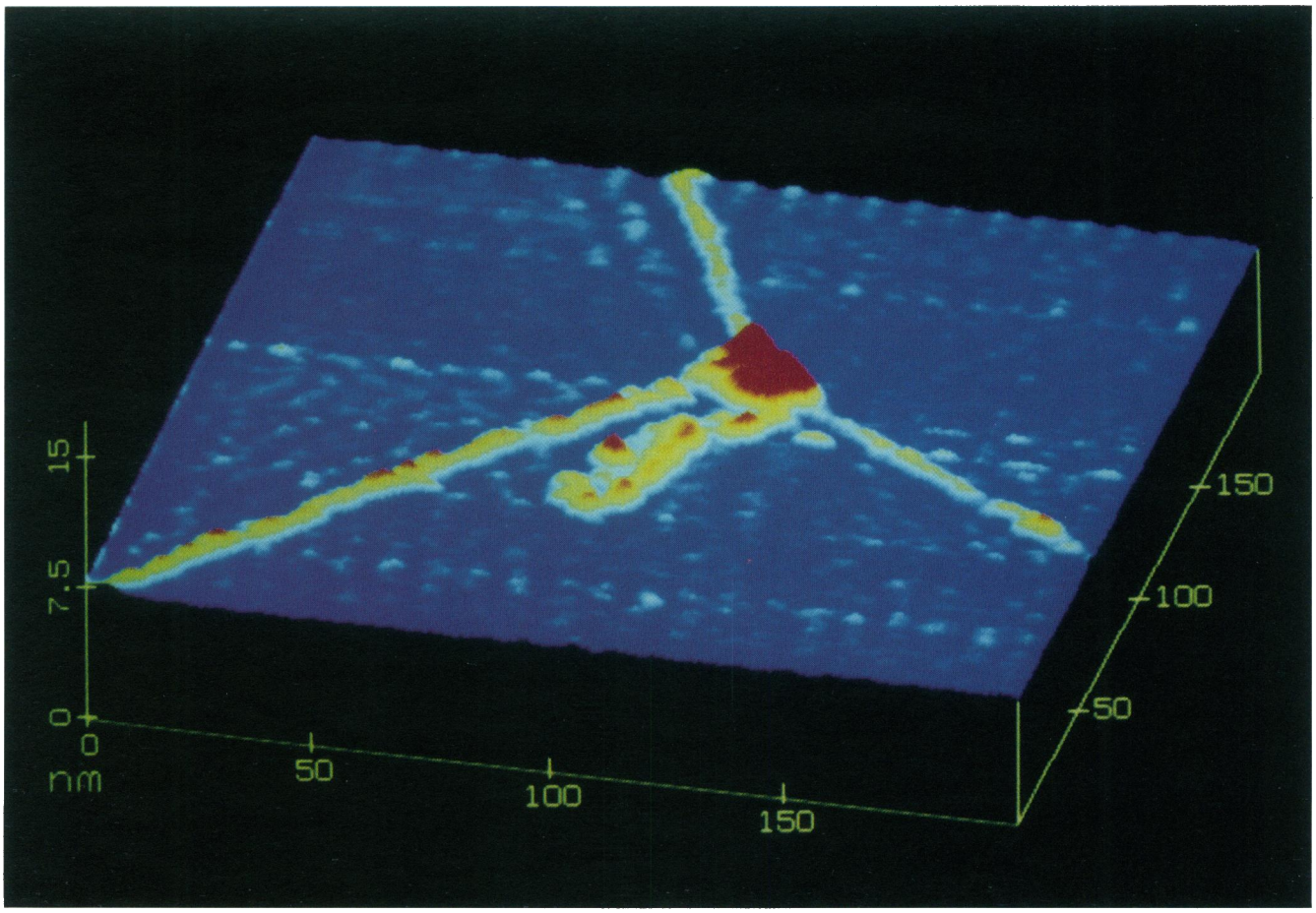

FIGURE 5 A complex between phosphorylase kinase and phosphorylase *b*. The two proteins at a concentration of 0.1 mg/ml were dialyzed against a 10 mM imidazole buffer containing 100 μM $CaCl_2$ and 100 μM $MgCl_2$ then equal volumes mixed together and 0.5 μl applied to the pyrolytic graphite chip and dried under a stream of nitrogen.

ver. The diamond chips are mounted with the aid of an optical microscope, however, there is no way of knowing whether the tip is sharp enough or properly oriented to provide resolution at the submolecular level.

An AFM image of a phosphorylase tetramer shown in Fig. 3 is similar to that seen in our earlier STM visualizations. The two dimers in Fig. 3 have average dimensions of 11 × 5.5 × 7.5 nm compared to 11 × 5.7 × 1.6 for the STM images of a dimer (1) and the dimensions of 11 × 5.5 × 6.5 nm by electron diffraction (6), 11 × 5.5 × 6.2 by x-ray scattering (22) and 12.5 × 6.3 nm by electron microscopy (no thickness measured) (23). The AFM images appear to agree perfectly with the sizes obtained by other techniques in two dimensions and vary by only 15% in the third.

In addition to individual dimers and tetramers, with STM we have often seen linear arrays of phosphorylase *b* that are 11 nm wide with a repeat distance of 5.7 nm and that extend for several micrometers. Portions of such chains are shown in Fig. 4 and on the cover. These arrays are formed by aggregation of dimers, presumably during the drying process. The images shown here contains much more evidence of surface details than our earlier ones (1). Although such chains have not yet been seen in physiologically active structures, the high concentrations of phosphorylase in the glycogen particle (~2–4 mM) would enhance the possibility of such aggregate forming. Electron microscopy studies have shown that dissolving crystals of phosphorylase *a* yield aggregates of parallel dimers that are at least 6–10 dimers long (6). In any case, the propensity of phosphorylase to form linear arrays on the graphite surface has proved useful in our study of the enzyme's structure and its metabolic interactions. In electron microscope studies of phosphorylase *b* crystals, chains of what appear to be tetramers found with a repeat distance of 12.5 nm are seen side by side to form the

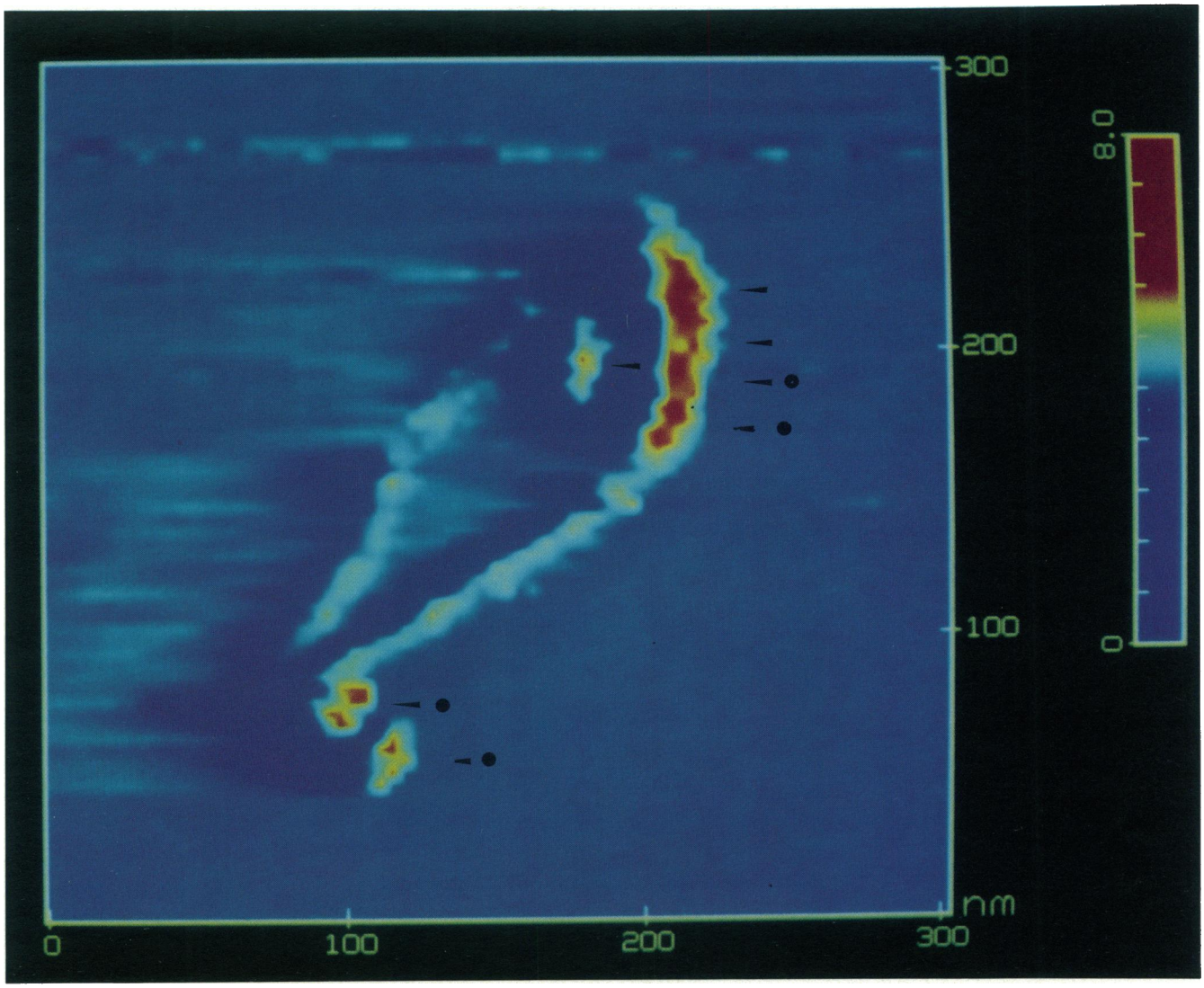

FIGURE 6 A second set of complexes between phosphorylase kinase and phosphorylase *b*. In this case several phosphorylase kinase molecules are associated with a chain of phosphorylase *b* dimers. The arrows point to individual complexes and the circles denote those complexes that were sufficiently distinct to measure (see text).

two-dimensional surface of the crystal (23). The dimer–dimer interface was parallel to the individual chains. Subsequent x-ray diffraction studies show that this sort of tetramer of phosphorylase *b* is composed of two dimers joined at their surfaces where the glycogen storage sites are located (24). In the chain shown in Fig. 4, there is no evidence of a tetrameric subunit and it appears that the dimer–dimer interface is perpendicular to the chain. Identification of the ligand binding sites on the STM images will require a comparison of the STM data with the crystallographic data as well as direct imaging of ligand bound to phosphorylase; both studies are underway. Because the phosphorylase in muscle is bound to glycogen at its glycogen storage site, the tetramers formed during crystallization at high concentrations of 5′AMP-Mg or IMP are of questionable physiological significance. Whether the chains formed on graphite and seen by STM have physiological relevance remains to be seen.

We next wished to explore the possibility of directly viewing enzyme substrate complexes of phosphorylase kinase and phosphorylase *b*. Complexes between the two enzymes were prepared by mixing 1:5 molar ratios of phosphorylase kinase and phosphorylase *b*. The total protein concentration of 0.1 mg/ml was a compromise, high enough to maximize the possibility of finding com-

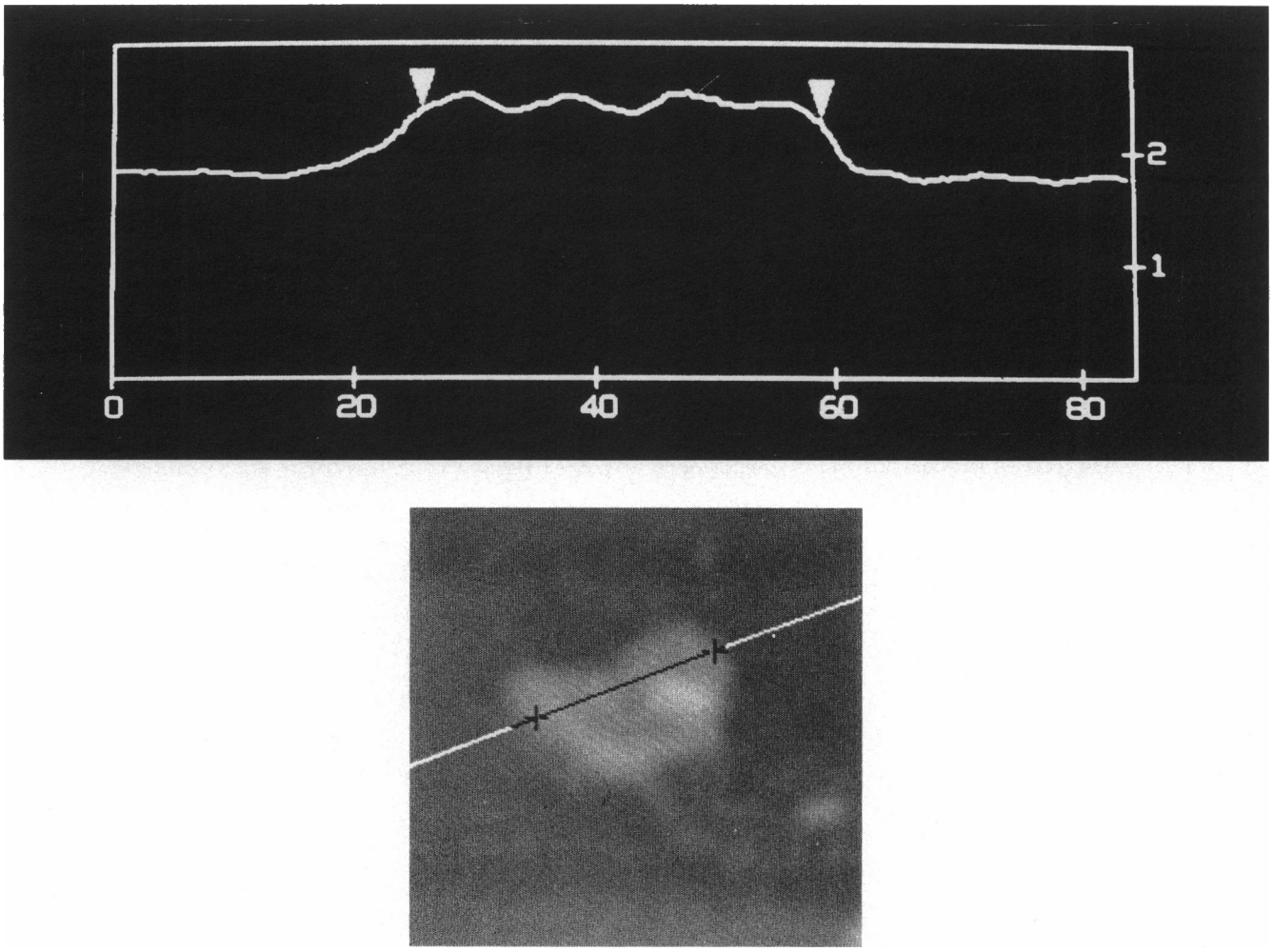

FIGURE 7 (*A*) A cross section of a single phosphorylase kinase molecule adsorbed to the graphite surface. (*B*) A cross-section of the phosphorylase kinase molecule in Fig. 4 bound to phosphorylase *b*. In both cases the units of dimension are nanometers.

plexes on the graphite surface but low enough to minimize nonspecific denaturing aggregation of the phosphorylase kinase.

Fig. 5 shows the STM image of a complex formed between a single phosphorylase kinase molecule and four phosphorylase *b* aggregates of the type observed previously (1). Three of the phosphorylase *b* chains clearly connect with the phosphorylase kinase and are linear with the longest extending over 1 μm across the graphite surface toward the lower right in the photograph. The other chains which are toward the lower and upper left also extend for $\sim$1 μm. Profiles taken perpendicular to each of the three linear chains yielded widths between 11 and 12 nm. The fourth phosphorylase *b* aggregate, positioned below the phosphorylase kinase molecule in Fig. 5 represents a condensed structure of the type described previously (2). A second type of complex containing several phosphorylase kinase molecules is shown in Fig. 6. Six phosphorylase kinase molecules are imaged as indicated by the arrows. In each case, the phosphorylase kinase molecules appear to be oriented with the junctions of their two lobes perpendicular to the phosphorylase *b* chain.

Comparison of the images of phosphorylase kinase in the isolated and complexed state shows that this molecule undergoes significant change in its size and shape on binding to its substrate, phosphorylase *b*. The phosphorylase kinase molecule shown in Fig. 5 has a somewhat smaller footprint on the graphite than the free enzyme (Table 1). The maximum width across the lobar junction of the complex was 32 nm compared with the range of 35–37 for the free form. The maximum dimension parallel to the junction is 23 nm (26–27 nm for the uncomplexed form). The maximum height, however, increased

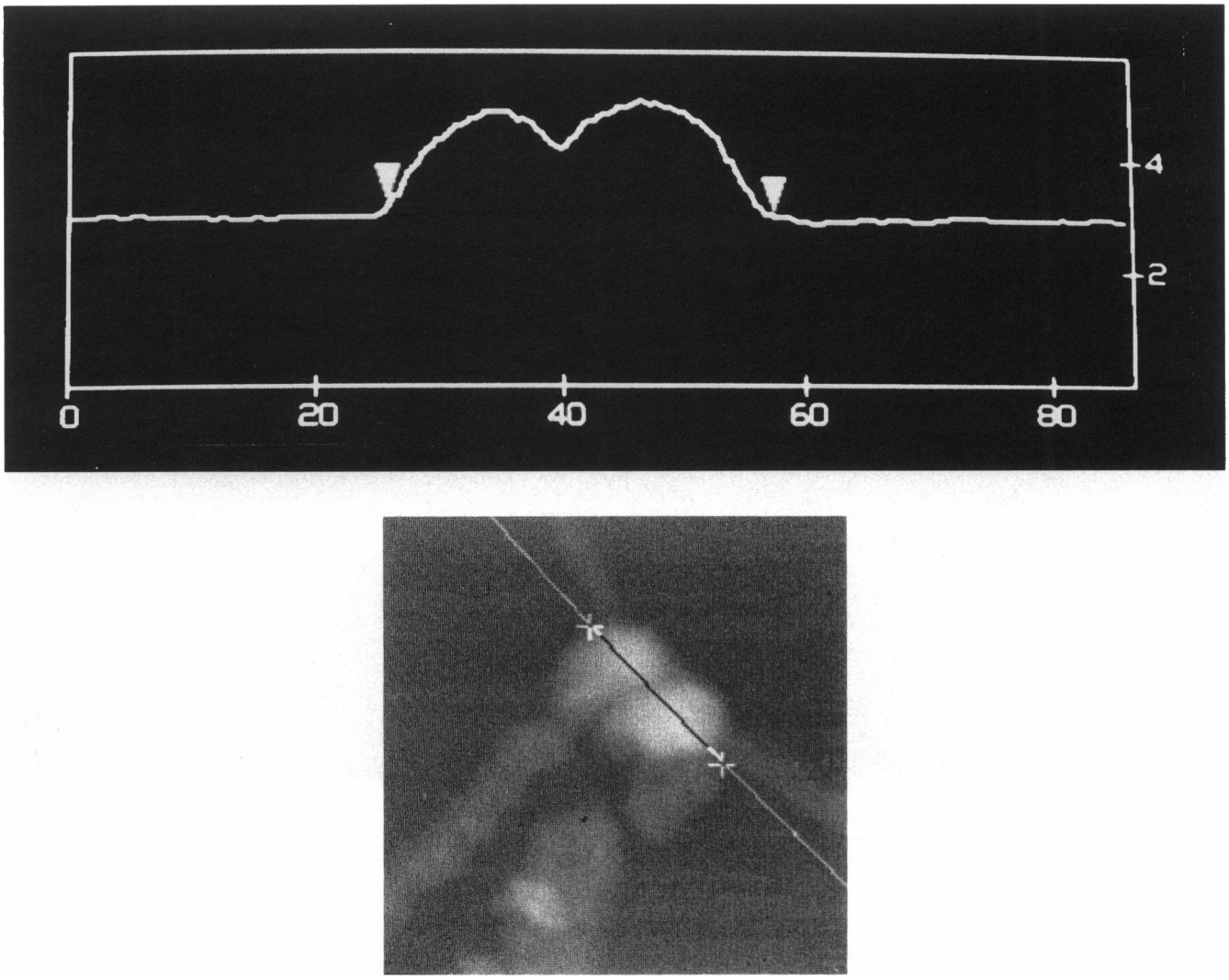

FIGURE 7 (continued)

to 2.3 nm from a range of 0.61 to 0.72 for free phosphorylase kinase. By measuring the height and width of several cross sections it was possible to estimate a volume for the complex. That value, 1,100 nm^3, is double that of the free enzyme (540 nm^3). Assuming there are four phosphorylase *b* molecules attached to the kinase, as indicated in Fig. 5, one can add an incremental value for the four phosphorylase *b* dimers. This was calculated based on an 11 × 5.7 nm dimer footprint (1) and the thickness of 1.6 nm reported above. That increment is 400 nm^3 giving a calculated value for a complex between one phosphorylase kinase and four phosphorylase *b* dimers of 940 nm^3. Although image resolution was not as great, the four complexes in Fig. 6 marked with circles at the arrows were measured. The average dimensions were 29 nm (27–30) by 20 nm (19–22) by 1.7 nm (1.5–2.1). The average volume was 990 nm^3 (870–1,150). Refinements in measurement techniques and more data will provide better estimates of such volume changes and their relationships to binding stoichiometries. One must keep in mind that the apparent volumes measured by STM are about three times smaller than the real values due to the error in thickness measurement described above. Although the two proteins imaged in this work were measured by STM at 30% of their true height, other proteins must be measured by this technique before a generalized correction factor could be appropriately introduced. Besides apparent size changes, images of single phosphorylase kinase molecules adsorbed onto the graphite surface without phosphorylase *b* are much flatter in appearance

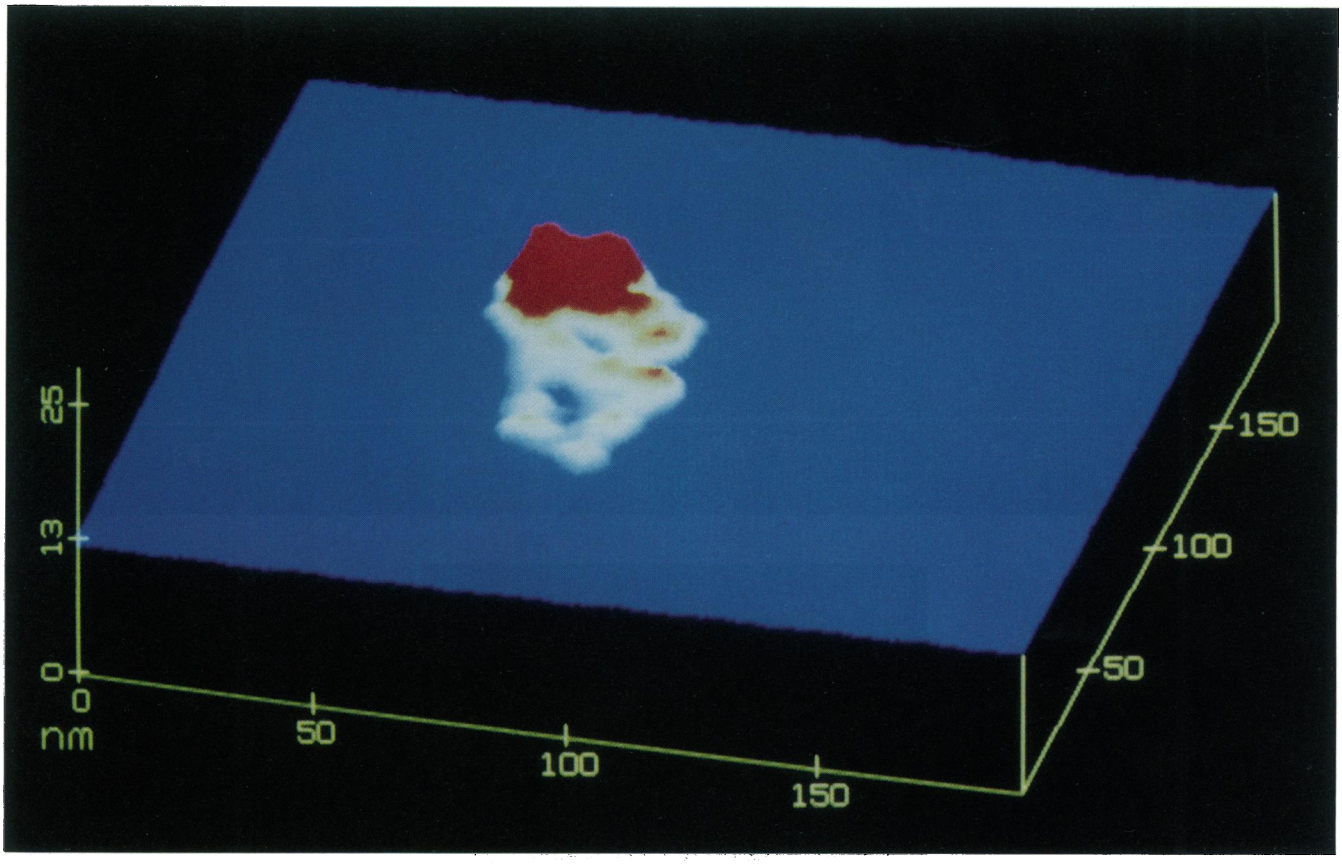

FIGURE 8 A complex between phosphorylase kinase and phosphorylase *b* viewed by AFM.

(Fig. 7 *A*) than those seen when the kinase is complexed (Fig. 7 *B*). When bound to phosphorylase *b*, the central depression between the two lobes of the kinase molecule becomes more prominent and appears as a large cleft.

An AFM image of a phosphorylase kinase molecule bound to an unorganized cluster of phosphorylase molecules is shown in Fig. 8. The dimensions of the kinase molecule are 33 × 26 × 5.5 nm; multiple cross section measurements gave a volume of 4,600 nm^3. Similar measurements of the phosphorylase tetramer in Fig. 3 yielded a volume of 350 nm^3 per dimer. Although one cannot see four distinct phosphorylase aggregates in this case, the binding stoichiometry should be the same as for the STM image. Four dimers of phosphorylase would have an apparent volume of 1,400 nm^3 by AFM which when added to the average AFM volume of phosphorylase kinase from Table 1 gives a predicted complex volume of ~5,000 nm^3, remarkably close to the measured volume of the complex.

An important issue to be considered in these studies is the possibility of the introduction of artifacts during the sample preparation. Because both STM and AFM are normally performed under conditions of room temperature and humidity and at atmospheric pressure it is not usual to use carefully dried specimens. They would soon equilibrate to the ambient condition. Several preliminary preparations of freeze-dried specimens did not produce better results. Freeze drying or critical point drying are necessary to preserve the structure of complex surfaces found on cells. Proteins, however, are molecules, held together by covalent and secondary bonding forces that are much stronger than those which maintain the integrity of cellular structure. Proteins are thus several orders of magnitude less sensitive to external forces such as ionic strength, pH, temperature, and surface tension. To gain an impression of the very high pressures induced by surface tension, it is useful to calculate the pressure on a drying sphere.[2] For a spherical protein 5 nm in diameter the pressure would be ~540 atm. Whereas cells such as erythrocytes are irreversibly modified when subjected to a

[2]The internal pressure of a sphere of water at 20°C due to surface tension can be calculated from the equation described in 1805 by Pierre Simon, Marquis de LaPlace (31): $\Delta p = 2 \times \gamma/r$, where γ is the surface tension of water (72.5 mJ m^{-2}) and r is the radius.

pressure of only 5 atm (25) proteins remain essentially unaffected at pressures up to several thousand atmospheres. Lactic dehydrogenase from a thermophilic bacterium showed no changes in its quaternary structure or catalytic function at pressures up to 2,800 atm (26). At 1,000 atm the unit cell of a lysozyme crystal was compressed ~0.6% (27). At 2,000 atm immunoglobulin light chains in solution did not unfold and showed volume changes of < -100 ml/mol (28). Human apolipoprotein A-I showed a volume change of -50 ml/mol at 3,000 atm and was not inactivated by that treatment (29). For phosphorylase kinase with a molar volume of 9.6×10^5 ml, a -100 ml/mol change would represent a 0.01% decrease in volume. For phosphorylase the maximum expected change would be on the order of 0.1%. Because the volume of a prolate spheroid is a function of the second power of the minor axis length, the degree of flattening would be even less than the volume change. Clearly the high pressures caused by surface tension can be expected to have little or no effect on a protein molecule. A direct study of drying forces on small objects showed that while empty virus coats (nucleic acid removed) and polystyrene spheres were flattened during air drying, neither intact virus particles nor ribosomes were distorted by that process (30). Macromolecules such as proteins are much more stable to physical forces than complex structures such as viruses and ribosomes. We propose that the surface tension forces associated with air drying of the samples is not sufficient to significantly distort protein molecules.

In conclusion, we have shown that scanning tunneling microscopy can be used to observe changes in protein shape when phosphorylase kinase binds its substrate, phosphorylase *b*. The images also provide information about the spatial relationships between the two enzymes in the complex. Neither crystallization nor elaborate sample preparation was needed to obtain the images presented here. Co-crystallization of phosphorylase *b* and phosphorylase kinase could provide a complex for x-ray diffraction studies, but the possibility of producing such crystals is remote. Even if such a complex could be caused to crystallize, its size ($M_r = 1.7 \times 10^6$) is well beyond the present range of crystallographic analysis. Atomic force microscopy, while providing direct molecular thickness measurements, does not yet have the ability to resolve structural features at the same level as STM. Both techniques are relatively simple to use and the instrumentation is inexpensive compared to electron microscopes or x-ray diffraction facilities. The STM-AFM combination may be the method of choice for estimating the sizes and shapes of proteins and their complexes.

This work was supported by the Minnesota Medical Foundation, the American Diabetes Association—Minnesota Affiliate, the National Institutes of Health (GM34341), the National Science Foundation (DCB-8719317), and the Center for Interfacial Engineering, a National Science Foundation Engineering Research Center.

Received for publication 1 June 1990.

REFERENCES

1. Edstrom, R. D., M. H. Meinke, X. Yang, R. Yang, and D. F. Evans. 1989. Direct observation of phosphorylase kinase and phosphorylase b by scanning tunneling microscopy. *Biochemistry.* 28:4939–4942.
2. Elings, V. B., R. D. Edstrom, M. H. Meinke, X. Yang, R. Yang, and D. F. Evans. 1990. Direct observations of enzymes and their complexes by scanning tunneling microscopy. *J. Vac. Sci. Technol.* A8:652–654.
3. Sprang, S. R., K. R. Acharya, E. J. Goldsmith, D. I. Stuart, K. Varvill, R. J. Fletterick, N. B. Madsen, and L. N. Johnson. 1988. Structural changes in glycogen phosphorylase induced by phosphorylation. *Nature (Lond.).* 336:215–221.
4. Trempe, M. R., G. M. Carlson, J. F. Hainfeld, P. S. Furcinitti, and J. S. Wall. 1986. Analyses of phosphorylase kinase by transmission and scanning transmission electron microscopy. *J. Biol. Chem.* 261:2882–2889.
5. Cohen, P. 1974. The role of phosphorylase kinase in the nervous and hormonal control of glycogneolysis in muscle. *Biochem. Soc. Symp.* 39:51–73.
6. Chignell, D. A., W. B. Gratzer, and R. C. Valentine. 1968. Subunit interaction in native and modified muscle phosphorylases. *Biochemistry.* 7:1082–1089.
7. Madsen, N. B. 1986. Glycogen phosphorylase. *In* The Enzymes. Vol. XVII. P. D. Boyer and E. G. Krebs, editors. Academic Press Inc., Orlando, FL. 365–394.
8. Pickett-Gies, C. A., and D. A. Walsh. 1986. Phosphorylase kinase. *In* The Enzymes. Vol. XVII. P. D. Boyer and E. G. Krebs, editors. Academic Press Inc., Orlando, FL. 395–459.
9. Koenst, M. H., J. S. Bishop, and R. D. Edstrom. 1985. Cross-linked phosphorylase b kinase–phosphorylase b complexes. *Fed. Proc.* 44:1074. (Abstr.)
10. Paudel, H. K., and G. M. Carlson. 1987. Inhibition of the catalytic subunit of phosphorylase kinase by its α/β subunits. *J. Biol. Chem.* 262:11912–11915.
11. Dimitrov, D. 1976. An investigation of direct interaction between phosphorylase kinase and phosphorylase-b. *Int. J. Biochem.* 7:529–533.
12. Tabatabai, L. B., and D. J. Graves. 1978. Kinetic mechanism and specificity of the phosphorylase kinase reaction. *J. Biol. Chem.* 253:2196–2202.
13. Farrar, Y. J. K., and G. M. Carlson. 1989. The steady-state kinetic mechanism of the catalytic subunit of phosphorylase kinase. *J. Cell Biol.* 107:281a. (Abstr.)
14. Binnig, G., H. Rohrer, Ch. Gerber, and E. Weibel. 1983. 7 × 7 Reconstruction on Si(111) resolved in real space. *Phys. Rev. Lett.* 50:120–123.
15. Binnig, G., C. F. Quate, and Ch. Gerber. 1986. *Phys. Rev. Lett.* 56:930–933.
16. Hansma, P. K., V. B. Elings, O. Marti, and C. E. Bracker. 1988. Scanning tunneling microscopy and atomic force microscopy:

application to biology and technology. *Science* (*Wash. DC*). 242:209–216.

17. Fischer, E. H., and E. G. Krebs. 1959. Muscle phosphorylase b. *Methods Enzymol.* 5:369–373.
18. Cohen, P. 1972. The subunit structure of rabbit skeletal muscle phosphorylase kinase and the molecular basis of its activation reactions. *Eur. J. Biochem.* 34:1–14.
19. Cantor, C. R., and P. R. Schimmel. 1980. Biophysical Chemistry. Part II. Techniques for the Study of Biological Structure and Function. W. H. Freeman and Co., New York. 846 pp.
20. Spong, J. K., H. A. Mizes, L. J. LaComb Jr., M. M. Dovek, J. E. Frommer, and J. S. Foster. 1989. Contrast mechanism for resolving organic molecules with tunnelling microscopy. *Nature* (*Lond.*). 338:137–139.
21. Lee, G., P. G. Arscott, V. A. Bloomfield, and D. F. Evans. 1989. Scanning tunneling microscopy of nucleic acids. *Science* (*Wash. DC*). 244:475–477.
22. Puchwein, G., O. Kratky, C. F. Golker, and E. Helmreich. 1970. Small-angle x-ray scattering measurements on rabbit muscle glycogen phosphorylase dimer B and tetramer B. *Biochemistry.* 9:4691–4698.
23. Eagles, P. A. M., and L. N. Johnson. 1972. Electron microscopy of phosphorylase b crystals. *J. Mol. Biol.* 64:693–695.
24. Barford, D., and L. N. Johnson. 1989. The allosteric transition of glycogen phosphorylase. *Nature* (*Lond.*). 340:609–616.
25. Halle, D., and S. Yedgar. 1988. Mild pressure induces resistance of erythrocytes to hemolysis by snake venom phospholipase A2. *Biophys. J.* 54:393–396.
26. Muller, K., T. Seifert, and R. Jaenicke. 1986. High pressure dissociation of lactate dehydrogenase from Bacillus stearothermophilus and reconstitution of the enzyme after denaturation in 6 M guanidine hydrochloride. *Eur. Biophys. J.* 11:87–94.
27. Kundrot, C. E., and F. M. Richards. 1987. Crystal structure of hen egg-white lysozyme at a hydrostatic pressure of 1,000 atmospheres. *J. Mol. Biol.* 193:157–170.
28. Herron, J. N., K. R. Ely, and A. B. Edmundson. 1985. Pressure-induced conformational changes in a human Bence-Jones protein (Mcg). *Biochemistry.* 24:3453–3459.
29. Mantulin, W. W., and H. J. Pownall. 1985. Reversible folding reactions of human apolipoprotein A-I: pressure and guanidinium chloride effects. *Biochim. Biophys. Acta.* 836:215–221.
30. Kellenberger, E., M. Haner, and M. Wurtz. 1982. The wrapping phenomenon in air-dried and negatively stained preparations. *Ultramicroscopy.* 9:139–150.
31. Heimenz, P. C. 1986. Principles of colloid and surface chemistry. Marcel Dekker, Inc., New York. 815 pp.